Role of Magnetic Geometry, Edge Flows and Electric Fields in Determining the L-H Transition Power Threshold

A. Y. Aydemir

Institute for Fusion Studies, The University of Texas at Austin, Austin, TX, USA

e-mail contact: aydemir@mail.utexas.edu

Abstract. The L-H transition power threshold, P_{LH}, is about a factor of two higher when the ion ∇B drift is away from the active X-point. A possible explanation was offered by the C-Mod group in terms of the effects of scrape-off-layer (SOL) flows, believed to be driven by turbulent processes with a strong ballooning character, on core rotation in L-mode. In a series of works, a complementary explanation for these flows was advanced by us that had its origin in the inability of Pfirsch-Schlüter currents to prevent charge-separation near the separatrix due to collisional effects. The resulting edge electric field, $\boldsymbol{E}_{PS}$, and the flows it drives were shown to have exactly the same symmetries as those observed on C-Mod, thus providing additional support for the C-Mod hypothesis regarding the power threshold. However, this "flow-centric" explanation for the dependence of P_{LH} on the drift direction is completely at odds with more recent DIII-D experiments where various combinations of co- and counter-injected neutral beams were used to drive toroidal rotation during the transition to H-mode; for every possible symmetry of fields and magnetic geometry, DIII-D observations on P_{LH} are opposite of what one would expect from the SOL-flow hypothesis. The resolution of this dilemma requires switching from the "flow-centric" view to one where, perhaps not surprisingly, the radial electric field is the relevant parameter. Using free-boundary equilibrium calculations, the flux surface average of the radial component of $\boldsymbol{E}_{PS}$ is shown to have a net negative (positive) value when the ∇B drift points towards (away from) the X-point. This observation alone can explain qualitatively the lower P_{LH} for these cases, since the L-H transition leads to a large negative E_r at the edge, which becomes easier to attain if the average $E_r < 0$ initially. Additionally, the toroidal flow generated by co (counter)-NBI makes a positive (negative) contribution to the background E_r. These observations imply that co-injected torque when the ion ∇B drift is in the "unfavorable" direction should result in the highest P_{LH}. The lowest would be with the drift in the direction of the X-point and counter-injection. Thus, the "E_r-based" viewpoint offers a uniform explanation for both the C-Mod and DIII-D results.

1. Introduction

It has been long recognized that the L-H transition power threshold, P_{LH}, shows an almost universal dependence on magnetic geometry. Transition to H-mode requires approximately a factor of two higher input power when the ion ∇B drift direction is away from the active X-point[1]. Although there is no definitive explanation for this observation yet, edge and scrape-off-layer (SOL) flows, and edge radial electric field are thought to play an important.

In an extensive study examining the edge flows in various magnetic geometries, the C-Mod group found a correlation between core rotation in L-mode discharges and the SOL flows that they attributed to turbulent transport with a strong ballooning character[2]. Starting with the general observation that the "intrinsic" toroidal rotation in H-mode is in the co-current direction, they concluded that the higher counter-current core rotation seen when the ion ∇B drift points away from the X-point requires a correspondingly higher input power to reverse it towards its "intrinsic" direction characteristic of H-mode discharges. Flows with very similar characteristics and symmetry properties were also seen in our magnetohydrodynamic (MHD) calculations[3, 4]; however, these were shown to have their origin in the inability of Pfirsch-Schlüter currents to completely short-circuit the electric field due to charge-dependent drifts in a torus because of collisional effects at the edge[5]. The exact form of this residual field is $\boldsymbol{E}_{PS} = \eta \boldsymbol{J}_{PS}$, where $\boldsymbol{J}_{PS}$ is the Pfirsch-Schlüter current and η is the edge resistivity. Fig. 1 presents a simplified picture of these currents, the resulting electric field, and the associated edge flows. Note that this effect is important only for the cooler and more collisional edge plasma, not in the core.

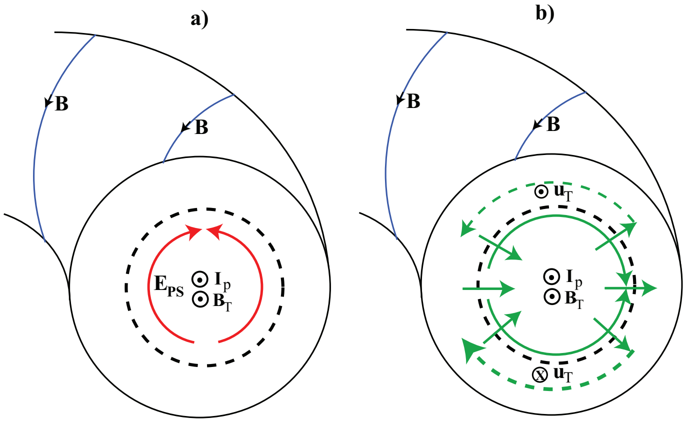

FIG. 1. a) A schematic description of the Pfirsch-Schlüter currents and the associated electric field (solid arrows) for a "normal" configuration of the plasma current and toroidal field. The currents are anti-parallel (to the field) on the high-field side, and parallel on the low-field side. b) Here the solid arrows represent the flows driven by the residual electric within the separatrix (the dashed circle). The dashed arrows outside the separatrix are the return flows in the SOL.

Unfortunately, this point of view where the SOL flows provide a boundary condition for the core rotation in L-mode, hereafter referred to as the "flow point of view," leads to incorrect expectations for P_{LH} when the effects of externally-driven toroidal rotation are included. For instance, by varying the balance between co- and counter-injected neutral beams, DIII-D showed that P_{LH} is lowest with counter-injected torque and increases as one moves through balanced to co-NBI, regardless of the magnetic topology[6, 7], in contradiction to the C-Mod interpretation of their results. In fact, as we will see in more detail in the next section, these torque-injection experiments on DIII-D contradict the implications of the "flow point of view" for P_{LH} in all possible permutations of plasma current, toroidal field, and the X-point location.

The resolution of this dilemma requires switching from this “flow point of view” to one where the radial electric field is the relevant parameter. Using free-boundary equilibrium calculations, we show that the flux surface average of the radial electric field associated with $\boldsymbol{E}_{PS}$ of Fig. 1 has a net negative value when the ∇B drift points towards the X-point. This observation alone can explain the lower P_{LH} for these cases, since the L-H transition leads to a large negative-E_r at the edge, which becomes easier to attain if $< E_r >$ is negative initially.

Note that this mechanism, namely collisional effects acting on the Pfirsch-Schlüter currents to generate a residual $\boldsymbol{E}_{PS}$, clearly is not the only source of electric field at the plasma edge. Shaing and coworkers used collisionless loss of trapped ions from a narrow layer within a poloidal ion gyroradius of the edge to explain the formation of a negative E_r well during the L-H transition[8, 9]. Similar direct loss mechanisms have also been studied in detail numerically[10] and analytically[11]. But these always lead to a negative E_r and lacks the symmetry properties of $\boldsymbol{E}_{PS}$ to account for the dependence of P_{LH} on the ∇B drift direction. Chang and coworkers (see Ref. [12] and the references therein) observe a similar E_r-well formation in their gyrokinetic simulations of the edge with the XGC code. In fact, in addition to a negative E_r near the separatrix, they observe a preferential loss of counter-current ions (with $v_\parallel < 0$) leading to an intrinsic source of co-current momentum source at the edge. They also find that, although the size of the loss-cone in velocity space is not affected much by the ∇B drift direction, the volume of real space from which the ions are lost is larger when it is in the favorable direction, thus implying a possible connection with the observed P_{LH} differences. This process and those generating $\boldsymbol{E}_{PS}$, the topic of this work, should complement each other. However, the formation of a field like $\boldsymbol{E}_{PS}$ appears to be excluded in XGC by the assumption of a potential constant on flux surfaces, $\phi = \phi(\psi)$.

2. The edge flows and radial electric field, and their symmetries

In a (ψ, θ, ζ) flux coordinate system with $\boldsymbol{B} = \nabla\psi\times\nabla\zeta + F\nabla\zeta$, where $\psi \equiv R^2(\boldsymbol{A}\cdot\nabla\zeta)$, and $F \equiv R^2(\boldsymbol{B}\cdot\nabla\zeta)$, the poloidal electric field resulting from the Pfirsch-Schlüter currents can be written as[5]

$$E_\theta = \eta q R^2 p' \left(1 - \frac{B^2}{\langle B^2 \rangle}\right). \tag{1}$$

Note that because of the sign convention adopted in the definition of $\boldsymbol{B}$ here, for a “normal” configuration where both the plasma current and toroidal field are in the positive $\nabla\zeta$ direction (clockwise when seen from above), $\nabla\psi$ points radially inward, $\nabla\theta$ is in the ion diamagnetic drift direction (clockwise in the poloidal plane of Fig. 1), and the safety factor $q < 0$. Thus, for a radially decreasing pressure profile, $p' > 0$, and $E_\theta > 0$ on the high-field side, as shown in Fig. 1. Reversal of the plasma current (or $\psi \to -\psi$) does not affect the sign of E_θ since both q and p' flip sign, but the reversal of toroidal field ($F \to -F$) results in $E_\theta \to -E_\theta$, as expected from the physical origin of this electric field.

A simplified projection of E_θ onto the poloidal plane is shown as a vertical field E_V in Fig. 2, which summarizes the symmetry properties of this electric field and the associated toroidal edge flows in all possible single-null configurations.

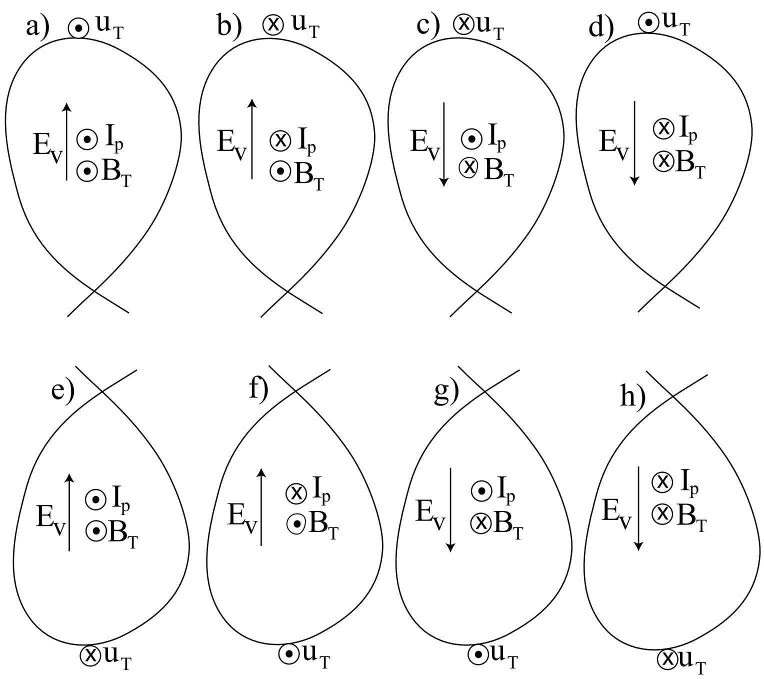

FIG. 2. Symmetries of the edge flows and the electric field arising from Pfirsch-Schlüter currents for all possible permutations of plasma current, toroidal field, and the X-point location. Note that E_V is in opposite direction to the ion ∇B drift and flips sign with the toroidal field. The toroidal velocity u_T, here a proxy for SOL flows, flips sign when either the plasma current or toroidal field is reversed, but not when both are reversed simultaneously (for fixed magnetic topology). A more extensive discussion of these symmetries can be found in Refs. [3, 4].

Note that E_V is non-uniform on a flux surface. In the simple geometry of Fig. 1, its radial component has a $\sin\theta$ variation in the poloidal direction. More generally, E_θ of Eq. 1 can be integrated numerically to obtain the potential ϕ and the radial electric field E_ψ on individual flux surfaces (this was done analytically for circular geometry in Ref. [5]):

$$\phi(\psi,\theta) = \phi(\psi,0) - \int_0^\theta E_\theta(\psi,\theta')d\theta', \quad E_\psi(\psi,\theta) = -\frac{\partial\phi}{\partial\psi}. \tag{2}$$

The integration constant is assumed to be zero for all flux surfaces, $\phi(\psi,0) = 0$. There is an unavoidable arbitrariness in this choice, but it is consistent with our earlier MHD calculations that had $E_\psi \sim -E_r \simeq 0$ at the outer midplane[3]. It is also consistent with this region being a plane of odd symmetry for the observed poloidal flows. Note that, like E_θ, $E_r \sim -E_\psi$ reverses only with the toroidal field. (The apparent change in E_ψ with reversal of I_p is deceptive, since it involves only a change in the direction of the unit vector.) Numerically obtained values for ϕ, E_ψ, and E_θ in a lower single-null (LSN) equilibrium are shown in Fig. 3.

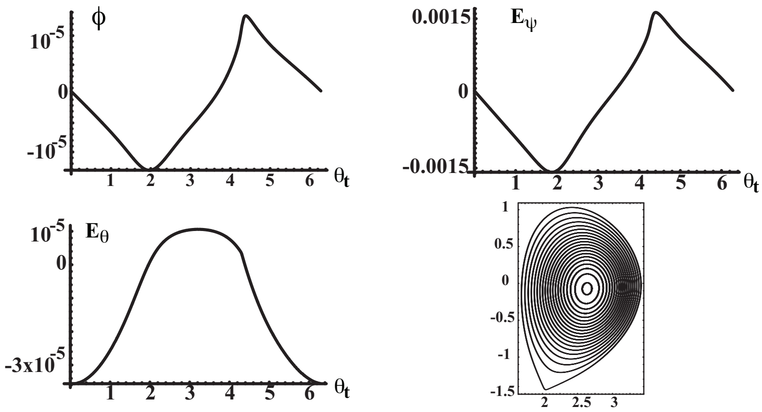

FIG. 3. Numerically obtained values (dimensionless) for the potential ϕ, radial electric field E_ψ ($E_\psi \sim -E_r$), and the poloidal electric field E_θ are shown for the $\rho = 0.995$ surface, where ρ is the normalized flux. The last panel shows the flux surfaces for a lower-single-null equilibrium used in the calculations. Here the angle θ_t increases in the counter-clockwise direction starting at the outer midplane; thus the X-point is at $\theta_t \sim 3\pi/2$.

Having established the basic characteristics of the edge flows and electric fields, we now return to DIII-D's torque-injection experiments and show why they tend to favor the edge radial electric field, rather than the edge flows, as the relevant parameter that determines P_{LH} differences for various magnetic geometries.

3. The role of edge flows vs. radial electric field in determining P_{LH} differences.

In the absence of the torque-injection experiments, the "flow point of view" mentioned in the Introduction provides a compelling explanation for the increase in P_{LH} when the ion ∇B drift points away from the X-point[2]: In panels (a), (b), (g), and (h) of Fig. 2, where the drift is in the favorable direction, the toroidal flow shown, a proxy for the dominant SOL flows, is in the co-current (intrinsic) direction. Thus, in L-mode, it already provides through the plasma boundary the seeds for an intrinsic rotation that fully develops after the transition to H-mode, which presumably becomes energetically easier to achieve under these conditions. In the remaining four panels, (c-f) of Fig. 2, the edge toroidal flow is in the counter-current direction, providing a boundary condition that opposes the intrinsic rotation of H-mode. Thus, starting with core rotation in the opposite direction, it becomes more difficult to achieve the requisite co-current flow of H-mode, leading to a higher input power requirement.

Unfortunately, DIII-D torque-injection experiments[6, 7] provide a completely contradictory point of view. By adjusting the mix of co- and counter-current neutral beam lines, these experiments established that induced co-current rotation results in the highest P_{LH}, which gradually decreases as the injected torque is varied towards counter-current, with an intermediate value for balanced beams (See Fig. 3 of Ref. [7]). This trend holds for both favorable and unfavorable ∇B drift directions.

Thus, although the configurations in panels (a), (b), (g), and (h) of Fig. 2 do have lower P_{LH}, this result cannot be due to the co-current boundary flow. Similarly, the higher P_{LH} expected for configurations in panels (c-f) cannot be explained in terms of the counter-current boundary condition provided by the SOL flows.

Clearly both the C-Mod and DIII-D experiments agree on when to expect lower/higher power thresholds, but the explanations offered completely contradict each other for all possible permutations of the plasma current, toroidal field, and X-point location. The resolution of this confusion may lie in switching the emphasis from the flows to the ambient or induced edge radial electric field as being the relevant parameter. To see how this shift in emphasis helps, consider the following observations:

- The L-H transition involves a deepening negative E_r well at edge[8, 9].
- Using the radial force-balance equation

$$E_r = \frac{1}{Z_i e n_i}\frac{\partial p_i}{\partial r} - v_{\theta i} B_\zeta + v_{\zeta i} B_\theta, \tag{3}$$

  it is easy to see that co-(counter-) current toroidal flow, $v_{\zeta i}$, makes a positive (negative) contribution to E_r. These two observations in combination are consistent with the DIII-D torque-injection results. In fact, counter neutral beam injection was known to lower the power threshold very early on (See Ref. [9] and the references therein).
- Although E_ψ of Eq. 2 varies poloidally on a flux surface (See Fig. 3), its flux-surface average, $\langle E_\psi \rangle$, is positive (implying a negative $\langle E_r \rangle$) when the ∇B drift is in the favorable direction (Panels (a), (b), (g), and (h) of Fig. 2). Similarly, $\langle E_\psi \rangle < 0$ ($\langle E_r \rangle > 0$) for the remaining panels with the unfavorable drift direction. Thus the lower P_{LH} when the drift is in the favorable direction can be attributed to this ambient radial electric field that is negative in an average sense. This variation of E_ψ is illustrated in Fig. 4 where $\langle -E_\psi \rangle \, / \, \langle |E_\psi| \rangle$ is plotted as the magnetic geometry is varied between LSN and USN configurations.

Thus, both the DIII-D torque-injection experiments, and the more general observations on P_{LH}'s dependence on the ∇B drift direction can be explained in terms of the ambient E_ψ of Eq. 2, and the contributions to it from driven toroidal flows. One more supporting evidence for the possibly central role that E_ψ plays again comes from DIII-D (See [13], Fig. 1(f)): In low-power L-mode plasmas, the radial electric field is positive when the drift is in the favorable direction for a LSN configuration, as in Fig. 2(a). It becomes negative when the toroidal field alone is reversed (Fig. 2 (c)). These observations are entirely consistent with the sign and symmetries of $E_r \sim -E_\psi$, assuming the experimental measurements are from at least slightly above the midplane.

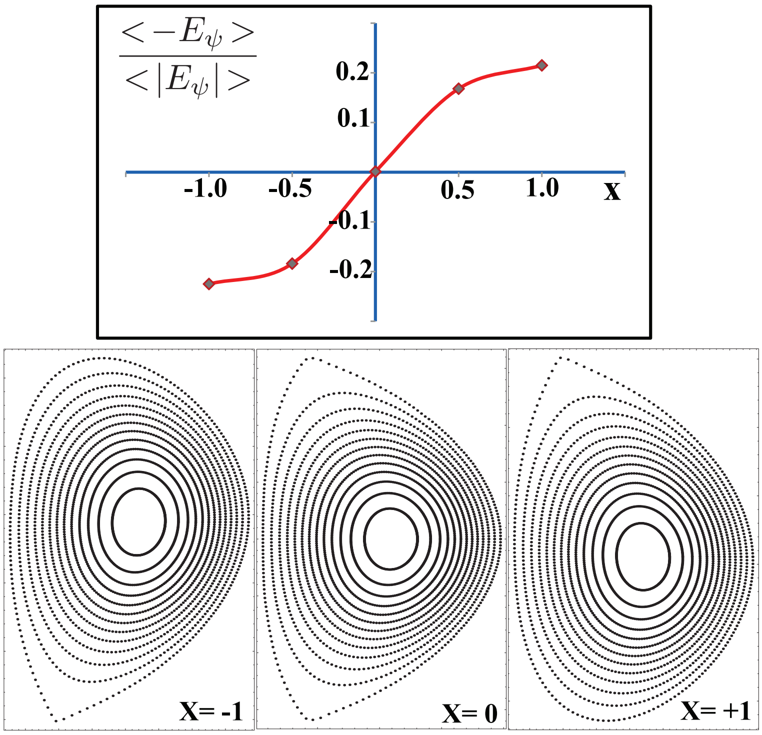

FIG. 4. Normalized flux-surface average of ($-E_\psi$) is plotted as the magnetic geometry is varied between a LSN and USN configuration. Here the variable x is a parameter that is used to continuously vary poloidal currents in the external coils to adjust the magnetic topology. Recall that $E_r \sim -E_\psi$.

4. Summary

Polarization of a toroidal plasma by charge-dependent drifts is generally assumed to be prevented by the Pfirsch-Schlüter currents. However, even for today's high-temperature plasmas, collisional effects close to the separatrix can lead to a residual electric field, $\boldsymbol{E}_{PS}$. In earlier works, the edge and SOL flows driven by this field were examined. Here the emphasis is on the radial electric field that can be associated with this process and its implications for the power threshold for the L-H transition in various magnetic geometries. We demonstrate that this field has the correct symmetries and characteristics to provide a unifying framework with which both the C-Mod edge flows and the results of DIII-D torque injection experiments can be explained.

Acknowledgment

This research was supported by the Office of Fusion Energy Science of the U.S. Department of Energy under Grant DE-FG02-04ER54742.

[1] F. Ryter and the H-Mode Database Working Group, Nucl. Fusion **36**, 1217 (1996).

[2] B. LaBombard, J. E. Rice, A. E. Hubbard, J. W. Hughes, M. Greenwald, J. H. Irby, Y. Lin, B. Lipshultz, E. S. Marmar, C. S. Pitcher, et al., Nucl. Fusion **44**, 1047 (2004).

[3] A. Y. Aydemir, Phys. Plasmas **14**, 056118 (2007).

[4] A. Y. Aydemir, Phys. Rev. Lett. **98**, 225002 (2007).

[5] A. Y. Aydemir, Nucl. Fusion **49**, 065001 (2009).

[6] D. J. Schlossberg, G. R. McKee, R. J. Fonck, K. H. Burrell, P. Gohil, R. J. Groebner, M. W. Shafer, W. M. Solomon, and G. Wang, Phys. Plasmas **16**, 080701 (2009).

[7] G. R. McKee, P. Gohil, D. J. Schlossberg, J. A. Boedo, K. H. Burrell, J. S. deGrassie, R. J. Groebner, R. A. Moyer, C. C. Petty, T. L. Rhodes, et al., Nucl. Fusion **49**, 115016 (2009).

[8] K. C. Shaing and E. C. Crume, Phys. Rev. Lett. **63**, 2369 (1989).

[9] K. C. Shaing, E. C. Crume, and W. A. Houlberg, Phys. Fluids B **2**, 1492 (1990).

[10] A. V. Chankin and G. M. McCracken, Nucl. Fusion **33**, 1459 (1993).

[11] K. Miyamoto, Nucl. Fusion **36**, 927 (1996).

[12] C. S. Chang and S. Ku, Phys. Plasmas **15**, 062510 (2008).

[13] T. N. Carlstrom, J. A. Boedo, K. H. Burrell, R. J. Colchin, C. Fenzi, R. J. Groebner, A. W. Leonard, G. R. McKee, R. A. Moyer, T. H. Osborne, et al., 27th EPS Conference on Contr. Fusion and Plasma Phys. **24**, 756 (2000).